Differential VASP phosphorylation controls remodeling of the actin cytoskeleton

Peter M. Benz[1,*,‡], Constanze Blume[1,*], Stefanie Seifert[2], Sabine Wilhelm[1], Jens Waschke[3], Kai Schuh[4], Frank Gertler[5], Thomas Münzel[6] and Thomas Renné[2,§]

[1]Institute of Clinical Biochemistry and Pathobiochemistry, [3]Institute of Anatomy and [4]Institute of Physiology, University of Würzburg, Würzburg, Germany
[2]Department of Molecular Medicine and Surgery, and Center for Molecular Medicine, Karolinska Institutet, Stockholm, Sweden
[5]Center for Cancer Research, Massachusetts Institute of Technology, Cambridge, MA, USA
[6]Second Medical Clinic, Department of Cardiology and Angiology, Johannes-Gutenberg-University, Mainz, Germany

*These authors contributed equally to this work
‡Present address: Institute of Physiology, University of Würzburg, D-97080, Würzburg, Germany
§Author for correspondence (thomas@renne.net)

Accepted 3 September 2009
Journal of Cell Science 122, 3954-3965 Published by The Company of Biologists 2009
doi:10.1242/jcs.044537

Summary

Proteins of the Enabled/vasodilator-stimulated phosphoprotein (Ena/VASP) family link signal transduction pathways to actin cytoskeleton dynamics. VASP is substrate of cAMP-dependent, cGMP-dependent and AMP-activated protein kinases that primarily phosphorylate the sites S157, S239 and T278, respectively. Here, we systematically analyzed functions of VASP phosphorylation patterns for actin assembly and subcellular targeting in vivo and compared the phosphorylation effects of Ena/VASP family members. Methods used were the reconstitution of VASP-null cells with 'locked' phosphomimetic VASP mutants, actin polymerization of VASP mutants in vitro and in living cells, site-specific kinase-mediated VASP phosphorylation, and analysis of the endogenous protein with phosphorylation-status-specific antibodies. Phosphorylation at S157 influenced VASP localization, but had a minor impact on F-actin assembly. Phosphorylation of the S157-equivalent site in the Ena/VASP family members Mena and EVL had no effect on the ratio of cellular F-actin to G-actin. By contrast, VASP phosphorylation at S239 (and the equivalent site in Mena) or T278 impaired VASP-driven actin filament formation. The data show that VASP functions are precisely regulated by differential phosphorylation and provide new insights into cytoskeletal control by serine/threonine kinase-dependent signaling pathways.

Supplementary material available online at
http://jcs.biologists.org/cgi/content/full/122/21/3954/DC1

Key words: Vasodilator-stimulated phosphoprotein (VASP), Ena/VASP family, Serine/threonine kinase, Actin turnover

Introduction

In cells, actin-filament-based structures control diverse activities such as polarized intracellular trafficking, cytokinesis, migration and adhesion (Mitchison and Cramer, 1996; Vasioukhin et al., 2000). Although cellular actin turnover is known to be spatially and temporally regulated by signaling cascades, many of the regulatory mechanisms remain to be characterized (Schmidt and Hall, 1998). Enabled/vasodilator-stimulated phosphoprotein (Ena/VASP) proteins localize to regions of dynamic actin remodeling and promote filament formation (Bear and Gertler, 2009; Trichet et al., 2008). In vertebrates, the evolutionary conserved protein family is comprised of VASP, mammalian Enabled (Mena), and Ena-VASP-like (EVL) (Krause et al., 2003; Kwiatkowski et al., 2003; Sechi and Wehland, 2004). All three proteins share a conserved structure consisting of an N-terminal Ena/VASP homology (EVH)-1 domain, a central poly-proline region (PPR) and a C-terminal EVH2 domain. Whereas the EVH1 domain mediates binding of Ena/VASP proteins to proline-rich ligands such as vinculin and zyxin (Ball et al., 2000), the PPR interacts with the actin-binding protein profilin and with Src homology 3 (SH3) domains (Benz et al., 2008; Lambrechts et al., 2000). Residues in EVH2 bind to G-actin and F-actin (Bachmann et al., 1999) and mediate tetramerization of Ena/VASP proteins (Kuhnel et al., 2004) (Fig. 1). In cells, Ena/VASP proteins promote F-actin assembly, which involves anti-capping (Barzik et al., 2005; Pasic et al., 2008), bundling (Applewhite et al., 2007; Bachmann et al., 1999; Kuhnel et al., 2004; Schirenbeck et al., 2006) and anti-branching (Bear et al., 2002; Skoble et al., 2001) activities.

The mammalian Ena/VASP proteins are known substrates of serine/threonine kinases, and human VASP harbors the three phosphorylation sites serine 157 (S157), serine 239 (S239), and threonine 278 (T278) (Blume et al., 2007; Butt et al., 1994; Gertler et al., 1996; Lambrechts et al., 2000). Whereas the first two phosphorylation sites are conserved in Mena, EVL contains only the first site (Fig. 1). In cells, the first and second site in VASP are phosphorylated in order by cAMP-dependent protein kinase (PKA). Conversely, cGMP-dependent protein kinase (PKG) initially phosphorylates the second site and then the first (Butt et al., 1994; Zhuang et al., 2004). Only recently, AMP-activated protein kinase (AMPK) was identified as the kinase responsible for phosphorylating T278 (Blume et al., 2007) (Fig. 1). VASP is dephosphorylated by protein phosphatase (PP)-1, PP2A, PP2B and PP2C (Abel et al., 1995), resulting in complex and dynamic phosphorylation patterns.

Evidence that phosphorylation might alter specific VASP properties has come from studies of phosphomimetic VASP mutants, which have one or all three phosphorylation sites substituted with acidic amino acids or alanine residues to imitate a permanently phosphorylated or unphosphorylated protein, respectively (Barzik et al., 2005; Geese et al., 2002; Grosse et al., 2003; Harbeck et al., 2000; Loureiro et al., 2002; Smolenski et al., 2000). Phosphorylation

affects the interaction of VASP with actin; however, the crucial phosphorylation sites and kinases involved are still unclear (Barzik et al., 2005; Harbeck et al., 2000; Laurent et al., 1999; Lindsay et al., 2007). VASP phosphorylation also modulates other protein-protein interactions. Whereas S157 phosphorylation abrogates interaction of VASP with the SH3 domains of Abl, nSrc and αII-spectrin (Benz et al., 2008; Lambrechts et al., 2000), binding of focal adhesion proteins to the EVH1 domain, and of profilin to the PPR, is independent of the VASP phosphorylation status (Ferron et al., 2007; Harbeck et al., 2000). Additionally, VASP phosphorylation status appears to modulate subcellular protein distribution. It has been postulated that VASP phosphorylation by PKA controls protein targeting to the cell-cell junctions of adherent cells (Benz et al., 2008; Comerford et al., 2002), but others have shown that PKG activity might control VASP localization (Lindsay et al., 2007; Smolenski et al., 2000).

In the present study, we analyzed VASP phosphorylation patterns for their impact on subcellular protein localization and actin filament assembly in cells and compared the phosphorylation-mediated regulation of VASP, Mena and EVL. We used a systematic strategy, combining phosphomimetic mutants, site-specific kinase-mediated phosphorylation and phosphorylation-status-specific antibodies. Our findings demonstrate that S157 phosphorylation controls subcellular VASP distribution, whereas phosphorylations at S239 and T278 impair F-actin accumulation. Similarly, the cellular F-actin to G-actin ratio was independent of the phosphorylation status at the S157 conserved site in Mena and EVL, whereas phosphorylation of the PKG homologous site in Mena interfered with F-actin assembly. This is the first comprehensive study of VASP phosphorylation that links serine/threonine-kinase signaling to F-actin levels in vivo.

Results

Ena/VASP phosphomimetic mutants imitate 'locked' phosphorylation patterns

Human VASP is a substrate for PKA, PKG and AMPK, which phosphorylate residues S157, S239 and T278, respectively. The first two phosphorylation sites are conserved in Mena (S236 and S376 in the murine protein), whereas EVL only contains the first site (S160 in the human protein) (Fig. 1A,C,E). We generated phosphomimetic Ena/VASP mutants by systematically exchanging phosphorylation sites for acidic amino acids to imitate a constitutively phosphorylated residue. Substitution with alanine arrested the remaining phosphorylation sites into a non-phosphorylated state. For VASP, constructs were denominated with a three-letter code according to the amino acids at positions 157, 239 and 278 (using A, alanine; D, aspartic acid; E, glutamic acid). For example, DAA is a VASP mutant bearing substitutions S157D, S239A and T278A. The phosphomimetic mutants covered all VASP

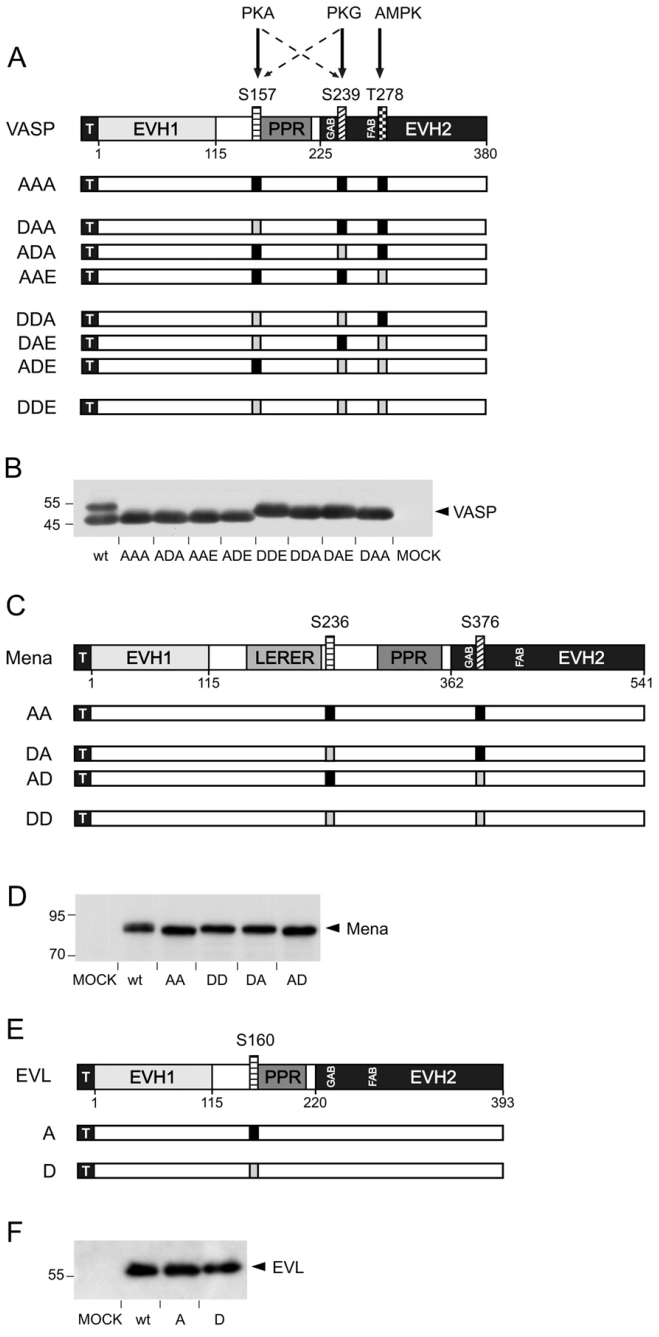

Fig. 1. Arrested phosphomimetic Ena/VASP mutants. (A) Domain organization and phosphorylation sites of N-terminally 6×His-tagged human wild-type VASP (wt) and phosphomimetic VASP mutants. VASP is composed of an N-terminal EVH1 domain, a PPR and a C-terminal EVH2 domain. The black square with white 'T' indicates the tag. PKA phosphorylates S157 (box shaded with horizontal lines) and S239 in order; S239 (box shaded with diagonal lines) is the primary target for PKG, which might also phosphorylate S157. T278 (box shaded with squares) is exclusively phosphorylated by AMPK. Phosphorylation sites were substituted with alanines (black boxes) or acidic residues (light boxes). Sites for G-actin binding (GAB, residues 234-237) and F-actin binding (FAB, residues 259-276), are located upstream of the preferred PKG and AMPK phosphorylation sites, respectively. The preferred PKA phosphorylation site is located upstream of the PPR. (B) Western blot with anti-6×His antibodies to confirm expression in EC_VASP$^{-/-}$ cells transiently transfected with cDNAs coding for VASP, arrested phosphomimetic mutants or vector without insert (MOCK). (C) Domain organization and phosphorylation sites of N-terminally 6×His-tagged murine wild-type Mena and phosphomimetic Mena mutants. LERER indicates the low complexity region harboring LERER repeats. Mena S236 and S376 correspond to VASP S157 and S239, respectively. Shading as for VASP. (D) Western blot with anti-6×His antibodies shows expression of wild-type and mutant Mena. (E) Domain organization and phosphorylation sites of N-terminally 6×His-tagged human wild-type EVL and phosphomimetic EVL mutants. EVL phosphorylation site S160 corresponds to VASP S157. (D) Western blot with anti-6×His antibodies confirms expression of wild-type EVL and arrested phosphomimetic mutants A and D. Note that (pseudo)phosphorylation at the first phosphorylation site leads to a mobility shift in SDS-PAGE of all mammalian Ena/VASP proteins.

phosphorylation patterns ranging from non-phosphorylated (AAA), single-phosphorylated (DAA, ADA, AAE), double-phosphorylated (DDA, DAE, ADE), up to triple-phosphorylated (DDE) proteins, each in a fixed state of phosphorylation (Fig. 1A). Mena and EVL constructs were named accordingly, using a two- or one-letter code for Mena or EVL, respectively (Fig. 1C,E).

It was previously shown that phosphorylation of VASP at S157, but not S239 or T278, leads to an electrophoretic mobility shift from 46 to 50 kDa in SDS PAGE (Butt et al., 1994; Krause et al., 2003; Kwiatkowski et al., 2003). We transfected microvascular endothelial cells from VASP-null mice (EC_VASP$^{-/-}$) with cDNAs coding for phosphomimetic mutants or wild-type protein and analyzed the migration of VASP variants by western blotting. Hexahistidine-tag-specific antibodies detected the characteristic doublet of S157 phosphorylated and non-phosphorylated wild-type VASP (Fig. 1B, lane 1). Phosphomimetic mutants with a negative charge substitution at position 157 (DDE, DDA, DAE, DAA; Fig. 1B, lanes 6-9) migrated with a higher apparent molecular mass (49-50 kDa) compared with mutants with alanine at this position (46 kDa; AAA, ADA, AAE, ADE; Fig. 1B, lanes 2-5). Similar to the phosphorylation of S239 and/or T278 in wild-type VASP (Blume et al., 2007), the migration of VASP mutants was not altered by the presence of acidic residues at the second or third phosphorylation site. Phosphorylation of Mena and EVL at their first phosphorylation sites also leads to a small shift in apparent molecular mass in SDS-PAGE (Gertler et al., 1996; Lambrechts et al., 2000). Phosphomimetic Mena and EVL mutants with an aspartic acid at the first phosphorylation site (Mena: DD and DA; EVL: D), migrated with a slightly higher apparent molecular mass than corresponding mutants with alanine at this position (Mena: AA and AD; EVL: A) (Fig. 1D and F). Expression levels of all Ena/VASP mutants were largely independent of the point mutations, as indicated by signal intensities in the western blots.

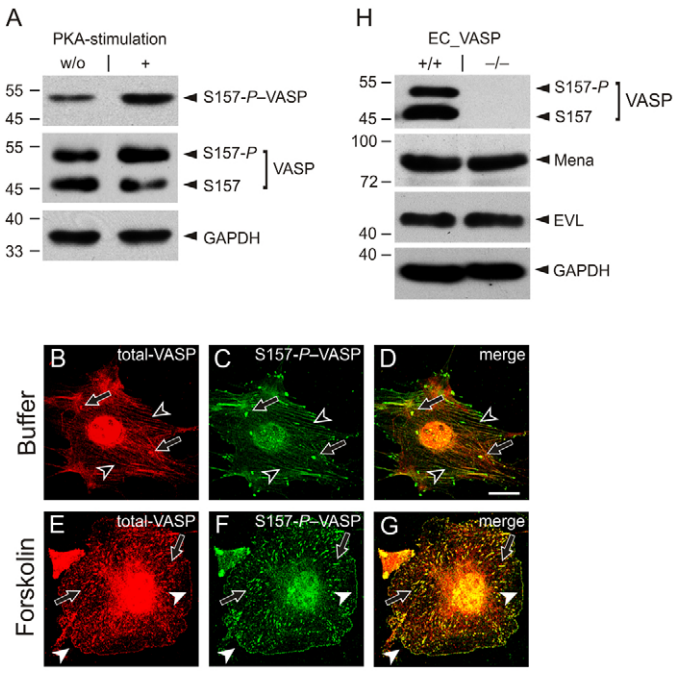

Fig. 2. VASP translocation to the cell periphery depends on S157 phosphorylation. Wild-type endothelial cells (EC_VASP$^{+/+}$) were incubated with forskolin (5 μM) or buffer and analyzed using antibodies against S157-*P*–VASP and total-VASP. (A) Western blots of cell lysates normalized for GAPDH. (B-G) Immunofluorescence images of fixed and permeabilized cells. The merge of total-VASP (red; B,E) and S157-*P*–VASP (green; C,F) is given in yellow (D,G). Black arrowheads indicate stress fibers, black arrows indicate focal adhesions, and white arrowheads indicate plasma membranes. Images were taken with a 100× objective and are representative of a series of eight experiments. Scale bar: 15 μm. (H) Comparison of VASP, Mena and EVL expression in EC_VASP$^{-/-}$ and EC_VASP$^{+/+}$ cells by western blotting. The cell lysates are normalized for GAPDH.

VASP targeting to the endothelial plasma membrane and focal adhesions depends on S157 phosphorylation

To analyze the impact of S157 phosphorylation on the localization of endogenous VASP, microvascular endothelial cells from VASP wild-type mice (EC_VASP$^{+/+}$) were treated with the PKA activator forskolin (5 μM) or buffer control. Forskolin increased S157 phosphorylation, as indicated by phospho-S157 (S157-*P*; also known as pS157)–VASP-specific antibodies (Fig. 2A, upper panel; S157-*P*) and anti-VASP antibodies (Fig 2A, middle panel; S157-*P*–VASP is the upper and S157-VASP the lower signal of the doublet) in western blotting. We compared the localization of total-VASP and S157-*P*–VASP in buffer- (Fig. 2B-D) and forskolin-treated EC_VASP$^{+/+}$ (Fig. 2E-G). In unstimulated cells, total-VASP (Fig. 2B) predominantly localized to stress fibers (black arrowheads) and small portions of total cellular protein enriched at punctuated structures, probably representing focal adhesions (black arrows). VASP at focal adhesions was strongly S157-phosphorylated and readily stained by phosphorylation-specific antibodies (Fig. 2C, black arrows). Both antigens co-localized at these sites (Fig. 2D). PKA-stimulation largely increased S157-*P* signal intensity and substantially changed the subcellular VASP distribution. Following a 10 minute forskolin treatment, total-VASP disappeared from stress fibers (compare total-VASP staining in stimulated versus unstimulated cells) and localized to focal adhesions (black arrows) and the plasma membrane (white arrowheads, Fig. 2E). VASP at these sites was S157-phosphorylated (Fig. 2F,G).

In addition to S157, PKA activation might also phosphorylate S239 and T278 (Butt et al., 1994) or modulate VASP localization by other pathways. Therefore, we confirmed the contribution of S157 phosphorylation to subcellular VASP targeting with a kinase-independent approach. VASP-deficient endothelial cells (EC_VASP$^{-/-}$) were reconstituted with phosphomimetic mutants. Except for VASP protein levels, EC_VASP$^{-/-}$ are indistinguishable from EC_VASP$^{+/+}$ and have similar Mena and EVL expression (Fig. 2H).

To analyze localization of phosphomimetic VASP mutants in EC_VASP$^{-/-}$, cells were transiently transfected with cDNAs coding for the eight VASP mutants AAA (Fig. 3A-C), DAA (Fig. 3D-F), ADA (Fig. 3G-I), DDA (Fig. 3J-L), AAE (Fig. 3M-O), DAE (Fig. 3P-R), ADE (Fig. 3S-U), and DDE (Fig. 3V-X). At 24 hours after transfection, cells were trypsinized and replated for 3 hours before fixing. Polyclonal anti-VASP antibodies were used for visualizing phosphomimetic mutants (green) and fluorescent phalloidin to stain for F-actin (red). For a semi-quantitative analysis of pseudophosphorylation-mediated VASP localization, two independent investigators determined the localization of mutants at the leading edge of lamellipodia or the accumulation at focal adhesions. VASP accumulation at these sites was scored weak (–), moderate (o) or strong (+) in >40 cells with mutant expression levels similar to endogenous VASP in EC_VASP$^{+/+}$ (Table 1). The VASP accumulation score was consistent with the length ratio of VASP-positive leading edges relative to the cell circumference. Mutants DAA, DDA, DAE and DDE (which share a negative

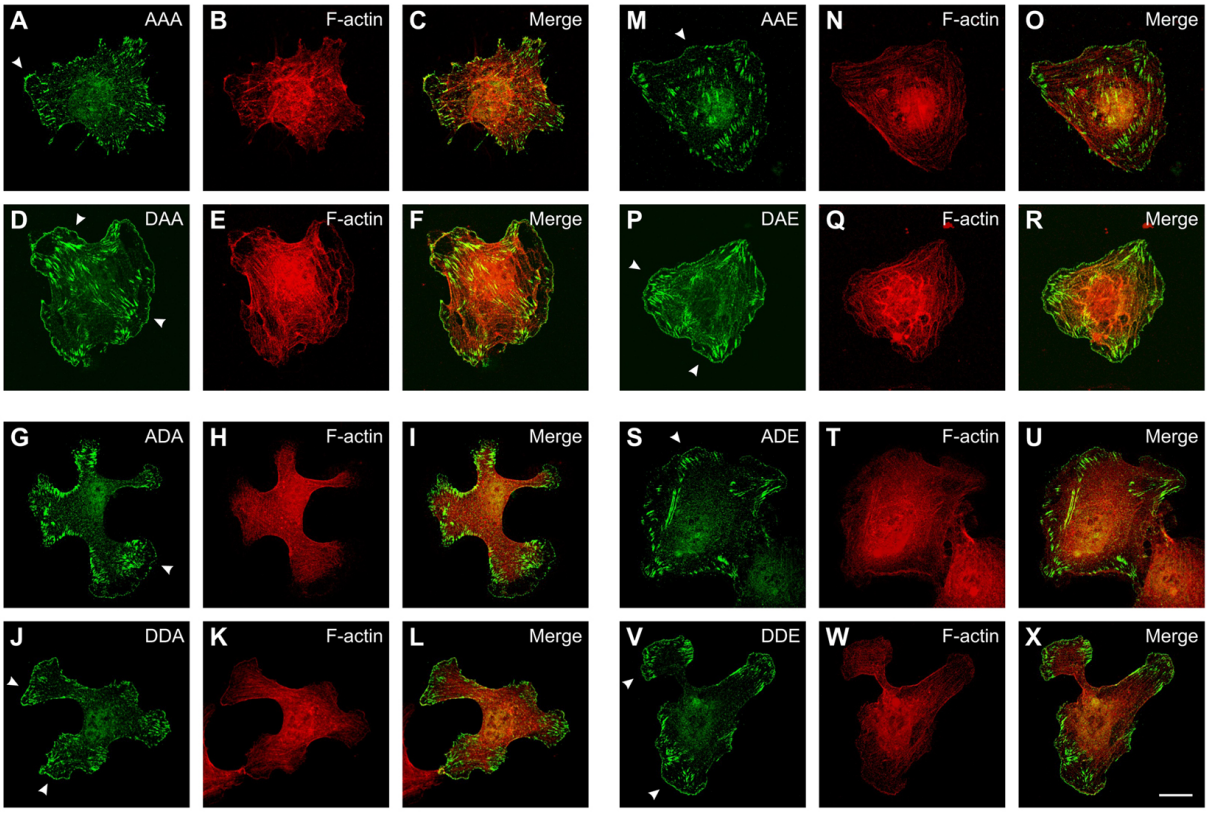

Fig. 3. Subcellular localization of phosphomimetic VASP mutants in EC_VASP$^{-/-}$ cells. Confocal immunofluorescence images of EC_VASP$^{-/-}$ transiently transfected with phosphomimetic VASP mutants AAA (A-C), DAA (D-F), ADA (G-I), DDA (J-L), AAE (M-O), DAE (P-R), ADE (S-U), and DDE (V-X). At 24 hours after transfection, cells were trypsinized and replated on gelatinized chamberslides for 3 hours before fixation and staining. Reconstituted VASP mutants were immunolocalized with anti-VASP antibodies (green) and F-actin with fluorescent phalloidin (red). Arrowheads indicate the leading edge of lamellipodia. Scale bar: 15 μm.

charge at the first site) were largely enriched at the leading edge of lamellipodia-like structures as compared with corresponding mutants with an alanine at this specific position (compare DAA vs AAA, DDA vs ADA, DAE vs AAE, and DDE vs ADE; Table 1 and Fig. 3, arrowheads). An acidic residue at position S157 also accumulated phosphomimetic mutants at focal-adhesion-like structures (compare DAA vs AAA, DDA vs ADA and DAE vs AAE; Table 1) and increased the number and size of focal adhesions.

In cells, VASP forms homotetramers but might also form heterotetramers with Mena and EVL (Bachmann et al., 1999; Grosse et al., 2003; Kuhnel et al., 2004; Loureiro et al., 2002; Vasioukhin et al., 2000; Zhuang et al., 2004). To exclude the possibility that tetramerization of transfected VASP mutants with

Table 1. Subcellular localization of phosphomimetic VASP mutants in EC_VASP$^{-/-}$ cells

VASP mutant	Lamellipodia	Focal adhesions
AAA	–	o
DAA	+	+
ADA	–	o
DDA	+	+
AAE	–	o
DAE	+	+
ADE	–	o
DDE	+	o

In EC_VASP$^{-/-}$ cells, subcellular localization of transiently expressed VASP mutants at the leading edge of lamellipodia and focal adhesions was scored as weak (–), moderate (o), or strong (+). 40 cells each with mutant expression levels similar to endogenous VASP in EC_VASP$^{-/-}$ were randomly selected and analyzed.

Table 2. Subcellular localization of phosphomimetic VASP mutants in MV^{D7} cells

VASP mutant	Lamellipodia	Focal adhesions
AAA	o	o
DAA	o	+
ADA	o	o
DDA	+	+
AAE	o	o
DAE	+	+
ADE	–	–
DDE	+	o

In MV^{D7} cells, subcellular localization of transiently expressed VASP mutants at lamellipodia or focal adhesions was scored as weak (–), moderate (o), or strong (+). Per mutant, 40 randomly selected cells with comparable VASP expression levels were analyzed.

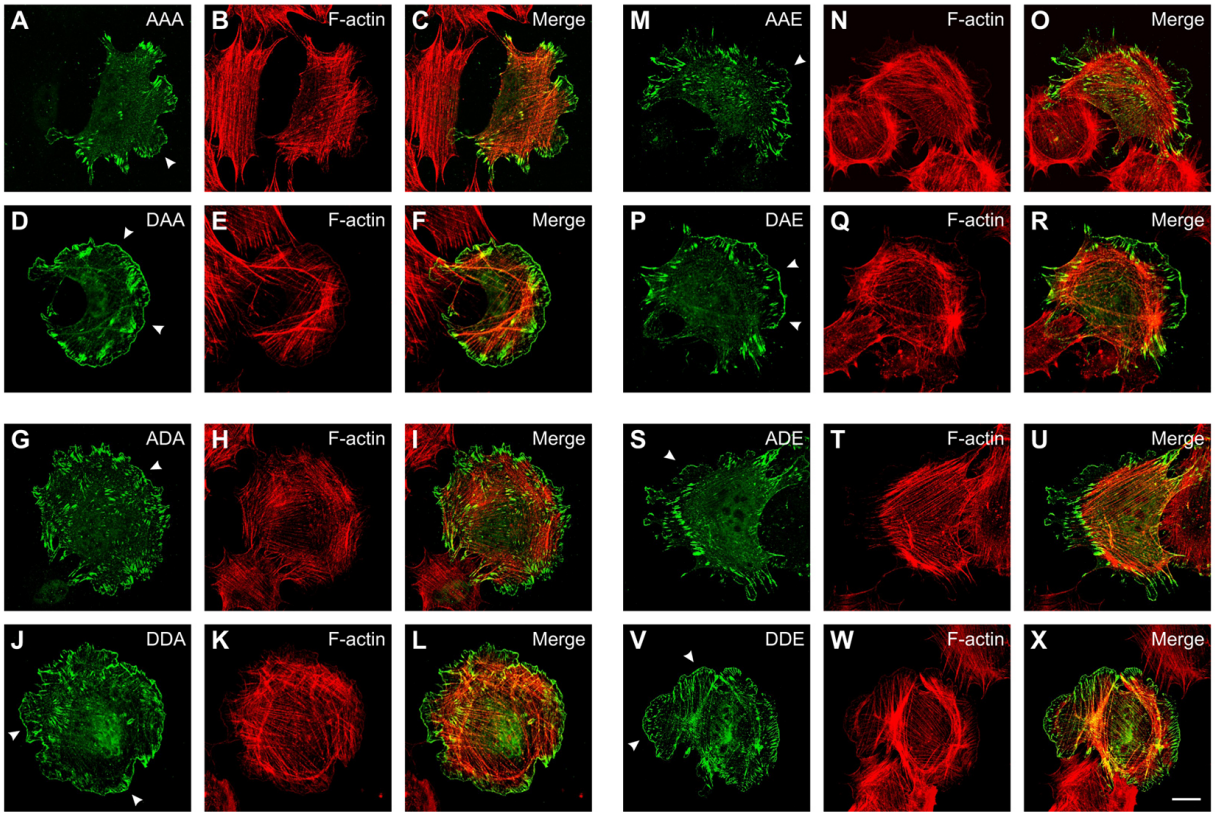

Fig. 4. Subcellular localization of phosphomimetic VASP mutants in MV^{D7} cells. Confocal immunofluorescence images of MV^{D7} cells transiently transfected with phosphomimetic VASP mutants AAA (A-C), DAA (D-F), ADA (G-I), DDA (J-L), AAE (M-O), DAE (P-R), ADE (S-U), and DDE (V-X). At 24 hours after transfection, cells were trypsinized and replated on fibronectin-coated chamber slides for 2 hours before fixation and staining. VASP mutants were immunolocalized with anti-VASP antibodies (green) and F-actin with fluorescent phalloidin (red). Arrowheads indicate the leading edge of lamellipodia. Scale bar: 15 μm.

endogenous Mena and EVL in $EC\_VASP^{-/-}$ (see expression of these family members in Fig. 2H) might modulate its localization, we analyzed the subcellular distribution of VASP mutants in MV^{D7} cells. MV^{D7} is a fibroblastic cell line derived from Mena/VASP double-gene-deficient mice, which expresses only trace amounts of EVL (Bear et al., 2000). MV^{D7} cells were transfected with phosphomimetic mutants, stained for VASP and actin as described for $EC\_VASP^{-/-}$, and mutant protein localization to lamellipodia or focal adhesions was scored 2 hours after attachment and spreading. Pseudophosphorylation of position 157 increased mutant localization at lamellipodia and focal-adhesion-like structures (Table 2 and Fig. 4; arrowheads indicate lamellipodia), with the exception of mutants AAA and DAA that were similarly enriched at lamellipodia. Localization of phosphomimetic VASP mutants was similar in MV^{D7} and $EC\_VASP^{-/-}$; however, the effect of pseudophosphorylation at position 157 on lamellipodia targeting was less pronounced in MV^{D7} than in $EC\_VASP^{-/-}$ (e.g. compare ADA and DDA in Tables 1 and 2). In $EC\_VASP^{-/-}$, mutant localization was largely independent of the phosphorylation status at the second and third sites, whereas pseudophosphorylation at these sites enhanced lamellipodia enrichment in spreading MV^{D7} cells (compare AAA vs DAA and ADE vs DDE in Tables 1 and 2), suggesting that cell-type- or cell-state-specific fine tuning of VASP localizations might exist. Together, immunolocalization of mutant and endogenous VASP indicate that (pseudo)phosphorylation of S157 enhances VASP targeting to lamellipodia and focal adhesions.

VASP pseudophosphorylation at S239 and T278 but not at S157 impairs VASP-driven F-actin accumulation in vitro

Previous studies indicated that phosphorylation interferes with VASP-driven actin polymerization in vitro (Barzik et al., 2005; Harbeck et al., 2000). To analyze all phosphorylation patterns systematically for their impact on F-actin assembly, we expressed the VASP pseudophosphorylation mutants in *Escherichia coli* and tested the purified proteins (Fig. 5A, inset) using in vitro actin polymerization assays. VASP does not initiate actin polymerization de novo under physiological salt conditions; however, in low salt, VASP interaction with actin can be used to measure actin nucleation (Barzik et al., 2005; Bear and Gertler, 2009). Monomeric actin (1 μM, 10% pyrene-labeled) was mixed with VASP (or VASP mutant, 0.25 μM each), and actin polymerization followed by an increase in pyrene fluorescence (Kouyama and Mihashi, 1981). In the absence of VASP, actin polymerization was slow, as indicated by a long lag phase and flat growth phase. A steady-state level of actin polymerization was not reached within 9 minutes (Fig. 5A; yellow curve, Actin). Addition of wild-type VASP or any of the phosphomimetic VASP mutants drastically increased actin polymerization, as indicated by a reduced lag phase and steep growth phase. For wild-type VASP, steady-state levels were reached in less than 1 minute, and the amount of F-actin at 1 and 9 minutes was 5.5- and twofold higher than in the absence of VASP, respectively (Fig. 5A; red curve, WT). Mutants AAA and DAA (Fig. 5A; green and magenta curves) enhanced actin polymerization to a similar extent as wild-type VASP, which is not serine/threonine-

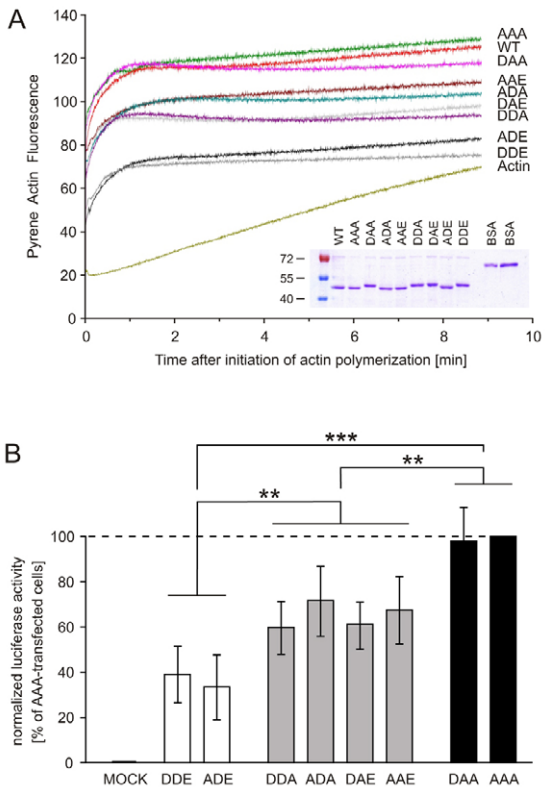

Fig. 5. VASP pseudophosphorylation at S239 and T278 but not at S157 impairs VASP-driven actin polymerization in vitro and in living cells. (A) In vitro actin polymerization driven by phosphomimetic VASP mutants. Pyrene-labeled G-actin (1 µM) was mixed with 0.25 µM purified recombinant wild-type (WT) or mutant VASP and the increase in fluorescence followed for 9 minutes. The curve labeled 'Actin' represents a reaction without VASP. A representative experiment of a series of five is shown. The inset shows a Coomassie-stained gel of purified wild-type and mutant VASP. A molecular mass standard is given on the left; 1 and 3 µg BSA per lane serves to calibrate the protein load. Acidic substitution at position 157 leads to a mobility shift of the constructs in SDS-PAGE. (B) SRE assay of HEK293 cells overexpressing phosphomimetic VASP mutants. Normalized luciferase activity in cells transfected with AAA or empty vector (MOCK) were assigned values of 100% and 0%, respectively. The normalized luciferase activity of the phosphomimetic mutants was grouped into three classes: black, grey and white bars corresponding to 0, 1 and 2 negative charges at either the second (S239) or third (T278) phosphorylation site, respectively. Bars represent the mean ± s.d. (n=9; ANOVA, $^{**}P$<0.01, $^{***}P$<0.001).

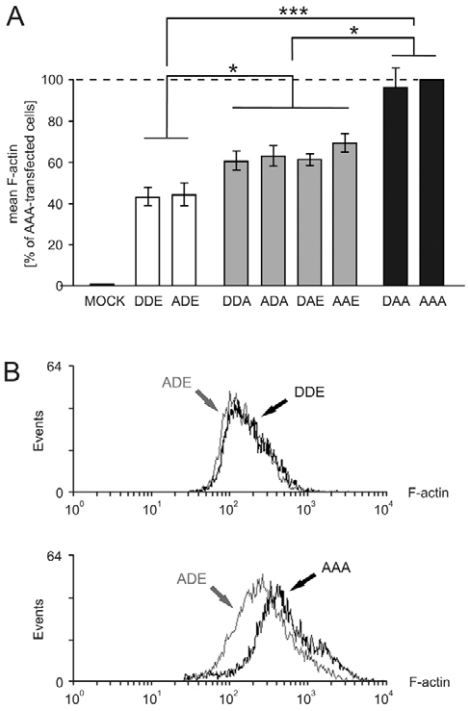

Fig. 6. F-actin determination in cells expressing phosphomimetic VASP mutant by FACS analysis. HEK293 cells were transiently transfected with cDNAs coding for the indicated VASP pseudophosphorylation mutants or empty vector. F-actin was stained with Alexa-Fluor-647-phalloidin and quantified using FACS-analysis. (A) F-actin content of cells transfected with AAA or empty vector (MOCK) was set to 100% and 0%, respectively. Bars represent mean ± s.d. (n=6; ANOVA, $^{*}P$<0.05, $^{***}P$<0.001). (B) Comparison of F-actin signals for ADE- (grey) versus DDE- (black, upper histogram) and ADE- (grey) versus AAA-transfected (black, lower histogram) HEK293 cells.

phosphorylated in *E. coli* (Blume et al., 2007). Mutants AAE, ADA, DAE and DDA were less effective in actin polymerization and the F-actin amount at 1 and 9 minutes was about 4.5- and 1.4-fold higher than without VASP, respectively (Fig. 5A; brown, cyan, light grey, and purple curves, respectively). Consistent with previous data (Harbeck et al., 2000), inhibition of actin polymerization conferred by pseudophosphorylation at the second site slightly exceeded inhibitory effects due to a negative charge at third site (ADA versus AAE and DDA versus DAE). In the assay, VASP mutants ADE and DDE displayed the lowest actin polymerization rates, and fluorescence was 3.5-fold higher than without VASP at 1 minute and almost identical to reactions without VASP at 9 minutes (Fig. 5A; black and grey curves, respectively). Together, the results support prior studies that analyzed the effects of VASP phosphorylation or pseudophosphorylation on F-actin levels in vitro (Barzik et al., 2005; Harbeck et al., 2000).

VASP pseudophosphorylation at positions 239 and 278 regulates global cellular F-actin content

To address the effect of VASP phosphorylation patterns systematically on F-actin accumulation in intact cells, we performed a serum response factor (SRF) transcriptional reporter assay (Fig. 5B). The assay quantifies the ratio of G-actin to F-actin by stimulation of SRF. This factor binds to the serum response element (SRE) and increases SRE-dependent expression of a luciferase reporter gene (Sotiropoulos et al., 1999). Therefore, the established reporter assay is a useful tool for quantifying the effects of actin-binding proteins of the Rho kinases (ROCK)-Lim kinase (LIMK)-cofilin pathway and to monitor filament assembly in living cells (Maekawa et al., 1999; Sotiropoulos et al., 1999). Transient VASP overexpression has been shown to induce F-actin assembly and SRE-driven luciferase activity (Grosse et al., 2003). We consistently found that the normalized luciferase activity of HEK293 cells overexpressing VASP mutants was markedly elevated over mock-transfected cells (control, set to 0%). Luciferase activity was maximal in AAA-transfected cells (set to 100%) and reached similar values in cells overexpressing DAA (98%; Fig. 5B). The activity of cells expressing DDA, ADA, DAE or AAE was significantly lower, ranging from 61 to 71%. Within this group, the SRE activity of mutants having a single negative charge at position 239 or 278 was not significantly different. Introducing a second negative charge at the second or third site further reduced F-actin formation, and SRE activity was minimal for the DDE and ADE mutants (39

and 34%, respectively; Fig. 5B). SRE activity driven by wild-type VASP varied from 49 to 81%, probably reflecting various non-defined phosphorylation patterns.

To confirm the effects of phosphorylation on F-actin assembly, we used quantitative fluorescence-activated cell sorting (FACS) (Fig. 6). The mean F-actin content of the cells expressing VASP mutants was measured relative to mock-transfected controls (0% value). The signal of the F-actin-specific dye, Alexa-Fluor-647-conjugated phalloidin, was normalized to the F-actin in HEK293 cells expressing the phosphorylation-resistant AAA mutant (100%). Overexpression of mutants DDA, ADA, DAE or AAE (which have a single negative charge either at position 239 or at 278) reduced the cellular F-actin amount to 60, 63, 61 and 68%, respectively; whereas DAA expression had a minor effect on actin fiber formation (97%). A second negative charge at positions 239 or 278 reduced F-actin formation to 44 and 47% (DDE, ADE; Fig. 6A). The F-actin signals in cells expressing DDE or ADE were almost identical (Fig. 6B, upper plot), but they differed in cells expressing ADE or AAA (Fig. 6B, lower plot). Together with the results from the pyrene-actin and SRE assays (Fig. 5A,B), the data demonstrate that pseudophosphorylation at positions 239 or 278 interferes with VASP-induced actin filament nucleation in vitro and F-actin accumulation in living cells, and that the inhibitory effects are additive and maximal in the 239/278 double-pseudophosphorylated mutants.

Pseudophosphorylation of Mena S376, but not Mena S236 or EVL S160, reduces F-actin levels in vivo

VASP pseudophosphorylations at the second and third site interferes with actin filament assembly in living cells (Fig. 5B, Fig. 6). Only the second site is conserved in Mena (S376), and EVL lacks equivalents to both sites (Krause et al., 2003) (Fig. 1). We investigated the function of Mena pseudophosphorylation for actin assembly using the SRE-reporter assay (Fig. 7A). Transient transfection only slightly increased the high endogenous Mena protein levels in HEK293 cells and degradation products appeared in overexpressing cells (supplementary material Fig. S1A). Therefore, we established the SRE assay in adherent CHO-S cells (Suzuki et al., 2006), which have no detectable endogenous Mena and allow high transient protein expression levels (supplementary material Fig. S1B). Normalized luciferase activity of CHO-S cells that overexpressed mutant Mena was markedly elevated over mock-transfected cells (control, set to 0%). Luciferase activity was maximal in mutant AA-transfected cells (set to 100%) and reached similar values in cells overexpressing DA variant (96%; Fig. 7A). The activity of cells expressing mutants AD and DD, which have a negative charge at the 376 position, was significantly lower and reached 39 and 38%, respectively. Luciferase activity induced by EVL A mutant (set to 100%) in HEK293 cells clearly exceeded levels of mock-transfected cells (control, set to 0%) and was almost identical to EVL D variant (99%; Fig. 7B).

S157 phosphorylation does not affect global cellular F-actin content

The previous findings in this study suggest that the pseudophosphorylation status of S157 is important for VASP localization in spreading cells but does not affect overall F-actin content. By contrast, pseudophosphorylation at positions 239 or 278 inhibits the VASP-dependent F-actin accumulation, but has a minor impact on subcellular targeting. To test this for kinase-mediated VASP phosphorylation, we used partially arrested mutants SAA, ASA and AAT (Fig. 8A). The mutants restrict phosphorylation to the first, second or third site, respectively, with the other sites blocked from phosphorylation. Using unstimulated reconstituted EC_VASP$^{-/-}$ cells, mutant SAA but not ASA or AAT migrated as a doublet in SDS-PAGE, indicating that S157 phosphorylation is blocked in ASA and AAT but partially phosphorylated in SAA (Fig. 8B). To investigate the consequences of PKA-mediated S157 phosphorylation on F-actin assembly, we used the SRE-based reporter assay (Fig. 8C). Overexpression of SAA induced F-actin assembly in unstimulated HEK293 cells (102%), similar to the level observed in AAA-transfected cells. By contrast, overexpression of ADE reduced the signal to 33% (positive control). Treatment of SAA-transfected cells with forskolin (5 μM) largely increased S157 phosphorylation, which was almost undetectable in unstimulated cells, as shown by S157-*P*-specific antibodies (Fig. 8D, upper panel). The relative signal intensities of the SAA doublet indicated that more than 75% of total SAA protein was phosphorylated at S157 (Fig. 8D, lower panel, anti-VASP). However, luciferase activity was not significantly changed by PKA stimulation for up to 80 minutes (99-107% versus 102%, n.s.; Fig. 8C), which was consistent with cells expressing DAA (98%). Higher forskolin concentrations or alternative PKA-activators, such as 8-Br-cAMP, did not affect SRE signals (not shown). Together, these results strongly suggest that PKA-mediated VASP S157 phosphorylation does not affect global F-actin content in cells.

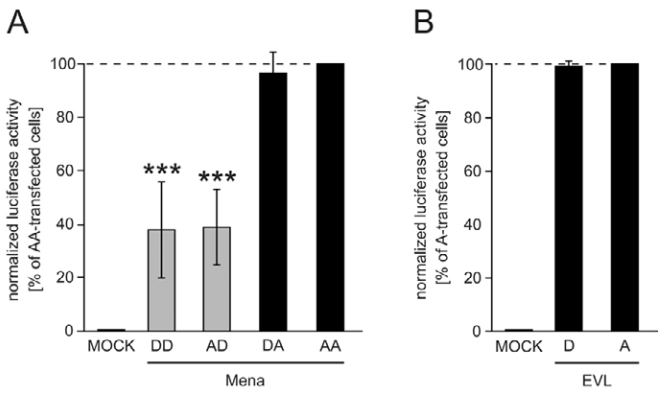

Fig. 7. Effect of Mena and EVL pseudophosphorylations for actin assembly in cells. (A) SRE assay of CHO-S cells overexpressing phosphomimetic Mena mutants. Normalized luciferase activity in cells transfected with AA or empty vector (MOCK) were assigned values of 100% and 0%, respectively. Mean values ± s.d. are given (n=13; ANOVA, *** P<0.001). (B) SRE assay of HEK293 cells transfected with EVL mutants D and A. Normalized luciferase activity in cells transfected with A or empty vector were assigned values of 100% and 0%, respectively. Mean ± s.d. (n=8; ANOVA, P>0.05 D versus A).

Phosphorylation at S239 and T278 impairs cellular F-actin accumulation in vivo

Next, we analyzed the effects of PKG-mediated VASP phosphorylation using SRE assays in HEK293 cells (Fig. 8E,F). In the absence of transfected PKG, the luciferase activity of cells expressing ADA and ADE served as a reference value and internal control, respectively (69 and 35% relative to the SRE signals of cells expressing AAA, set to 100%). Mutant ASA, with phosphorylation restricted to position 239, was co-transfected with

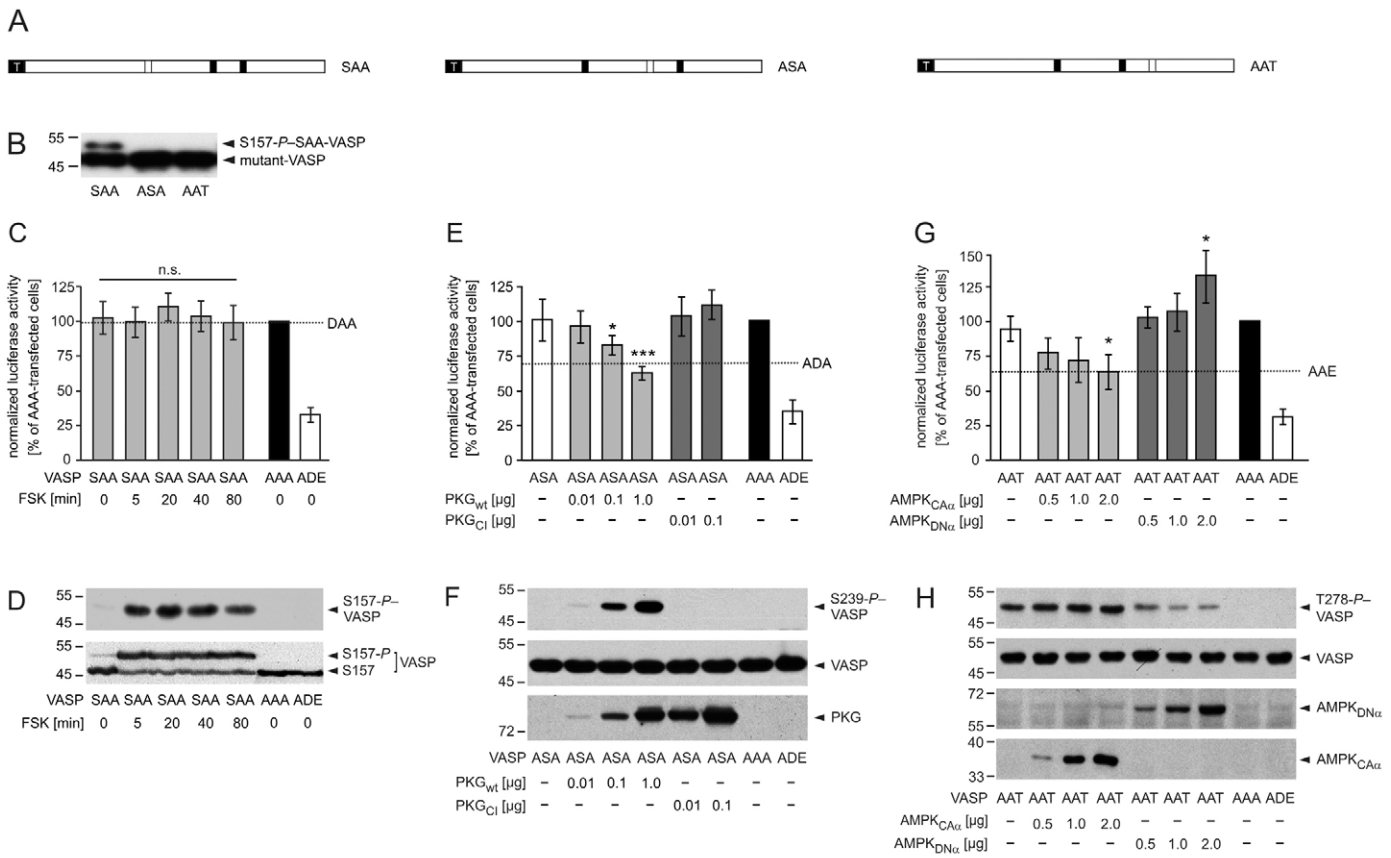

Fig. 8. Phosphorylation at S239 and T278 but not at S157 impairs VASP-driven actin polymerization in living cells. (A) Schematic representation of partially arrested VASP mutants. To analyze defined VASP phosphorylation patterns, we substituted two of the three phosphorylation sites with alanine residues, retaining one to allow kinase-mediated phosphorylation specifically at this residue. Black and open boxes indicate alanine and an accessible phosphorylation site, respectively. White 'T' indicates the tag. (B) Western blot with anti-VASP antibodies to confirm expression of mutants SAA, ASA or AAT in transfected EC_VASP$^{-/-}$ cells. (C-D) PKA-mediated phosphorylation of S157-VASP does not affect global cellular F-actin content. Transfected HEK293 cells were incubated with forskolin (FSK, 5 µM) for 5, 20, 40 and 80 minutes. (C) SRE assay. The luciferase activities in cells transfected with AAA or empty vector (MOCK) were set to 100% and 0%, respectively. For comparison, the luciferase activity of unstimulated cells expressing DAA is given (dashed line, n=6; ANOVA, P>0.05 stimulated versus unstimulated SAA-transfected cells). The transfection with ADE, which maximally blocked VASP-driven actin assembly (Fig. 5B), served as a positive control. (D) The expression of VASP mutants and phosphorylation of SAA at S157 was confirmed by immunoblotting using antibodies against S157-*P* (upper panel) and total-VASP (lower panel). (E-F) PKG-mediated VASP phosphorylation at S239 reduces global actin polymerization. HEK239 cells were co-transfected with VASP mutant ASA and the indicated amounts of PKG_{wt} or PKG_{CI}. (E) For comparison, the signal of unstimulated cells expressing ADA is given (dashed line). Normalized luciferase activities are plotted relative to the activity in cells transfected with AAA or empty vector (MOCK) (set to 100% and 0%, respectively; n=8; ANOVA, *P<0.05, ***P<0.001). ADE served as a positive control. (F) Anti-S239-*P* antibodies indicated the phosphorylation of S239-ASA (upper panel) in western blots. The expression of VASP mutants in transfected cells was confirmed by immunoblotting with anti-VASP antibodies (middle panel). The expression of PKG variants was probed using antibodies against PKG (lower panel). (G-H) AMPK-meditated phosphorylation of VASP at T278 interferes with F-actin assembly. HEK239 cells were transiently co-transfected with VASP-AAT and $AMPK_{CA\alpha}$ or $AMPK_{DN\alpha}$. (G) For comparison, the activity of AAE-transfected cells is indicated (dashed line). Normalized luciferase activities are plotted relative to the activity in cells transfected with AAA or empty vector (MOCK) (set to 100% and 0%, respectively; n=8; ANOVA, *P<0.05). ADE served as a positive control. (H) Western blots using anti-T278-*P* (upper panel) and anti-VASP antibodies (second panel) confirmed T278 phosphorylation and AAT expression, respectively. AMPK variants were probed by myc-tag specific antibodies (lower panels).

plasmids coding for wild-type (PKG_{wt}) or a catalytically inactive forms (PKG_{CI}) of PKG. Kinase activity was abolished in PKG_{CI} by an A405K substitution (Smolenski et al., 2000). Western blotting with S239-*P*-specific antibodies revealed that co-expression of PKG_{wt} increased ASA phosphorylation in a dose-dependent manner concomitant with a significant decrease in luciferase activity to 61%, compared to ASA without PKG (101%). By contrast, co-expression of PKG_{CI} and ASA increased SRE signals slightly, but not significantly (103 and 110% of AAA; Fig. 8E) in transfected cells. To address the function of AMPK-mediated phosphorylation at residue T278 in F-actin formation, we co-expressed mutant AAT with either a constitutively active ($AMPK_{CA\alpha}$) or a dominant negative ($AMPK_{DN\alpha}$) form of the AMPK α1-subunit (Fig. 8G,H). Consistent with basal phospho-T278 (T278-*P*; also known as pT278)–VASP levels in endothelial cells (Blume et al., 2007), T278-*P*-specific anti-VASP antibodies detected T278-phosphorylated AAT mutants in the absence of transfected AMPK (Fig. 8H, upper panel, lane 1). The luciferase activity in these cells was slightly lower than in AAA controls (92 versus 100%). The co-expression of increasing amounts of $AMPK_{CA\alpha}$ with AAT increased T278-*P*-levels and reduced SRE signals down to 61% in a dose-dependent manner, which was similar to the reduction observed in cells expressing AAE (62%, comparative value). By contrast, a reduction of T278-*P* levels by $AMPK_{DN\alpha}$ expression increased SRE signals up to 133% in a dose-dependent manner. The data is consistent with the results obtained

with the phosphomimetic mutants and demonstrates that phosphorylation at S239 and T278 interferes with global F-actin assembly in cells.

Discussion

Originally, VASP was identified in platelets as a substrate for cyclic-nucleotide-dependent protein kinases PKA and PKG (Halbrugge et al., 1990). Its strategic localization at the intersection of important kinase-driven signaling cascades established phospho-VASP as a marker for the integrity of cyclic-nucleotide-dependent pathways in cardiovascular cells. Today, analysis of phospho-VASP levels in platelets is used in clinical diagnostics (reviewed in Munzel et al., 2003; Gachet and Aleil, 2008). Despite its importance, the cellular function and complexity of VASP phosphorylation has remained uncertain.

VASP is a substrate of the protein kinases PKA, PKG and AMPK that primarily phosphorylate the sites S157, S239 and T278, respectively. Whereas the first two phosphorylation sites are conserved in Mena, EVL contains only the first site. In vitro studies have suggested that PKA-mediated VASP phosphorylation has a negative effect on both actin nucleation/G-actin binding and VASP interaction with actin filaments (Harbeck et al., 2000). In order to clarify underlying molecular mechanisms, we analyzed all VASP phosphorylation patterns systematically for their impact on actin filament assembly and subcellular protein targeting and compared phosphorylation-mediated effects of Ena/VASP family members. The study correlates defined VASP phosphorylation patterns with distinct functions in endothelial and HEK293 cells. The phospho-VASP-mediated regulation of actin dynamics appears to be of general importance and has been observed in endothelial cells (Benz et al., 2008; Price and Brindle, 2000; Rentsendorj et al., 2008; Rosenberger et al., 2007), leukocytes (Lawrence and Pryzwansky, 2001), platelets (Pula et al., 2006) and fibroblasts (Grosse et al., 2003), and in glioma (Zhuang et al., 2004), smooth muscle (Chen et al., 2004) and epithelial cells (Lindsay et al., 2007).

One of our key findings is that subcellular VASP localization is predominantly regulated by S157 phosphorylation in spreading endothelial cells. In the endothelium, VASP is involved in sealing cell-cell contacts and permeability regulation (Benz et al., 2008; Furman et al., 2007; Rentsendorj et al., 2008; Rosenberger et al., 2007; Schlegel et al., 2008). S157-*P* or pseudophosphorylated VASP was enriched at lamellipodia and focal adhesions in spreading cells (Figs 2, 3 and Table 1). The activation of PKA has been shown to increase S157 phosphorylation and to regulate VASP accumulation at the cell periphery in human (Comerford et al., 2002) and murine microvascular endothelial cells (Benz et al., 2008). The PKA-mediated phosphorylation of S157 blocks VASP binding to the SH3 domains of Abl (Howe et al., 2002), Src and αII-spectrin (Benz et al., 2008); interferes with complex formation; and coincides with S157-*P*–VASP accumulation at sites of high actin dynamics at the cell periphery. S157-*P*–VASP concentration in the cell periphery is also observed in platelets (Wentworth et al., 2006), in part due to PKCδ-mediated VASP phosphorylation (Pula et al., 2006). In addition to S157-*P*, previous studies have suggested a role of S239 phosphorylation for VASP localization. Thrombin-induced phosphorylation of AST, but not SAT, resulted in the translocation of VASP to the cell periphery in human umbilical vein endothelial cells (HUVEC) (Profirovic et al., 2005). By contrast, the stimulation of VASP S239 phosphorylation in the same cell line was shown to detach the protein from focal adhesions and to translocate it in the opposite direction, from the cell periphery to the cytosol (Smolenski et al., 2000). The two studies used different experimental conditions, making the results difficult to compare. Localization of our phosphomimetic mutants indicates that the phosphorylation of S239 and T278 has a minor effect on the subcellular distribution of VASP in endothelial cells (Fig. 3 and Table 1). However, cell-type-specific regulation of Ena/VASP proteins might exist because the phosphorylation status of S239 modulates VASP localization in renal epithelial cells in NO-dependent signaling pathways (Lindsay et al., 2007). Importantly, phosphorylation at S239 and T278 has significant effects on VASP interaction with G- and F-actin (Barzik et al., 2005; Harbeck et al., 2000) as well as on the ability of VASP to bind the chemotactic receptor CXCR2 (Neel et al., 2009).

We also analyzed VASP mutants in Ena/VASP-deficient fibroblasts and consistently found that mutant subcellular localization depends on the pseudophosphorylation status of S157 (MV^{D7}; Fig. 4 and Table 2). The localization of Mena mutants appeared to be independent of their pseudophosphorylation status in this cell line (Loureiro et al., 2002); however, the cells were analyzed under steady-state conditions rather than in spreading cells as in the current studies. MV^{D7} cells do not make filopodia and lamellipodia robustly once they are spread (Applewhite et al., 2007), and localization of actin-binding proteins might differ depending on the cytoskeleton turnover rate. Indeed, localization patterns of all phosphomimetic VASP mutants in MV^{D7} cells that were allowed to spread for 24 hours were indistinguishable (not shown), consistent with the previous literature (Loureiro et al., 2002).

In contrast to its role in subcellular targeting, VASP S157 phosphorylation had a minor impact on global cellular F-actin content (Fig. 5B, Figs 6 and 8), although this site might play an important role in regulating F-actin assembly at the plasma membrane (e.g. in lamellipodia or filopodia) or focal adhesions. The phosphorylation-independent recruitment of profilin–G-actin complexes (Harbeck et al., 2000; Reinhard et al., 1995) might explain the increased F-actin formation in cells expressing DDE or ADE as compared to mock-transfected cells, and the similar activities of DAA versus AAA and DDE versus ADE in the SRE and FACS assays (Fig. 5B and Fig. 6). In agreement with VASP S157 phosphorylation, phosphomimetic substitution of the conserved PKA site in Mena (S236) and EVL (S160) had minor effects on cellular F-actin content (Fig. 7).

Phosphorylation and phosphomimetic substitution of S239 and T278 synergistically impaired VASP-driven actin assembly in vitro (Fig. 5A) and in living cells (Fig. 5B, Fig. 6, Fig. 8E,G). Supporting the inhibitory role of S239- and T278-phosphorylation in VASP-driven actin assembly, Barzik and colleagues (Barzik et al., 2005) demonstrated that PKA-mediated phosphorylation of SAT or SSA reduced VASP-driven actin assembly. In their actin polymerization assay, the inhibitory effects on VASP anti-capping activity conferred by the phosphorylated VASP mutants were similar, suggesting that phosphorylation at S239 and T278 blocks VASP-driven actin assembly to a similar extent. In the presence of barbed-end capping proteins, blocking S157 phosphorylation did not affect phospho-VASP-regulated actin assembly. Together, the data suggest that phosphorylation at S239 and T278 decreases VASP anti-capping and F-actin bundling activity and impairs phospho-VASP-driven actin polymerization in vitro (Barzik et al., 2005). Notably, the S239 site is adjacent to the VASP G-actin binding site (residues 234-237), whereas T278 is adjacent to the F-actin binding site (residues 259-276) (Bachmann et al., 1999). Because actin filaments are negatively charged, VASP phosphorylation and phosphomimetic substitutions impair its ability to bind actin and cause a reduction in VASP-driven

actin filament assembly (Barzik et al., 2005), supporting our pyrene-actin, FACS and SRE-based data (Figs 5, 6 and 8). Consistently, pseudophosphorylation at the VASP S239 homologous site in Mena (S376) impaired F-actin accumulation (Fig. 7).

For fibroblast motility, the Mena phosphorylation status at the first site (S236; equivalent to S157 in VASP) is crucial. Though a phosphorylation-resistant Mena mutant (S236A) co-localized with wild-type protein, the mutant failed to rescue the hypermotile phenotype of MV^{D7} cells (Loureiro et al., 2002). By contrast, the inhibition of phosphorylation at the second site (S376A), which is preferred by PKG, restored the motility similar to that of transfected wild-type Mena, arguing against a role of PKG activity in phospho-Mena-driven actin-based processes, at least in the absence of more global regulation (Loureiro et al., 2002). It has been shown that *Drosophila* Ena, which lacks an equivalent to S157-VASP (Gertler et al., 1996), localizes properly but fails to complement the motility phenotype of VASP/Mena-null fibroblasts. However, findings from cell-motility models do not necessarily reflect the results from SRE-based systems. Interestingly, AMPK-mediated phosphorylation at T278-VASP is unique to the Ena/VASP protein family (Blume et al., 2007), allowing a more complex regulation of VASP than of Ena and Mena/EVL (Han et al., 2002).

In this study we focused on the three VASP phosphorylation sites S157, S239 and T278, which were originally identified by ^{32}P-peptide analysis of PKA-phosphorylated purified VASP (Butt et al., 1994). While this study was in progress, proteomic high-throughput screenings identified nine novel phosphorylation sites in VASP (Dephoure et al., 2008; Rikova et al., 2007; Zahedi et al., 2008) that might modify VASP functions. This is reminiscent of cortactin, another actin-binding protein, for which proteomic and transcriptomic analyses identified new serine/threonine phosphorylations and acetylations. Some of these sites are located within the F-actin-binding region of cortactin and, at least for acetylations, regulate interaction of the protein with actin filaments (Martin et al., 2006; Zhang et al., 2007). In VASP, the novel phosphorylation sites are located in the EVH1 domain (Y16 and Y39) and are clustered upstream of the tetramerization motif (residues 336-380) in the EVH2 domain (T316, S322, S323, S324, T327, T328, T335). Whether these sites are dynamically phosphorylated, and whether these phosphorylations regulate VASP functions, remains to be shown.

In summary, we have shown how VASP phosphorylation regulates VASP-driven actin filament formation and subcellular targeting of the protein in vivo. The PKG- and AMPK-mediated phosphorylation of VASP-S239 and VASP-T278, respectively, synergistically interferes with F-actin accumulation but has a minor impact on subcellular targeting. Only the PKG site is conserved in Mena, and phosphorylation at this position impairs Mena-driven actin-filament assembly. By contrast, the PKA site is conserved among all mammalian Ena/VASP family members (VASP S157, Mena S236 and EVL S160) and phosphorylation at this site does not affect Ena/VASP-driven F-actin assembly, but favors VASP localization to focal adhesions and lamellipodia as cells spread. Therefore, this study characterizes mechanisms by which Ena/VASP proteins connect serine/threonine-kinase signaling cascades with the actin cytoskeleton.

Materials and Methods

Plasmids and transfection experiments

The hexahistidine (6×His)-tagged Ena/VASP mutants were generated by site-directed mutagenesis using the QuikChange Multi kit (Stratagene) and designated with: (i) three capital letters representing the residues at positions 157, 239 and 278 in the human VASP protein in one-letter amino acid code; (ii) two capital letters representing the residues at positions 236 and 376 in the murine Mena protein; (iii) one capital letter representing the residue at position 160 in the human EVL protein. For example, VASP mutant AAE has the three mutations S157A, S239A and T278E. Point mutations were introduced using Ena/VASP cDNA in pcDNA3 vector (Invitrogen) and adequate primers (supplementary material Table 1). Wild-type and catalytically inactive (CI) forms of human PKGIβ (Sandberg et al., 1989) and myc-tagged constitutively active (CAα), dominant negative (DNα), or wild-type (wtα) forms of the AMPK α1-subunit were used as previously described (Blume et al., 2007; Woods et al., 2000). CAα is a truncated form of the wild-type αI-subunit (amino acids 1-312) containing a T172D mutation that mimics phosphorylation. Phosphorylation of T172 of the αI-subunit is essential for enzyme activity.

Cell culture

Immortalized endothelial cells from wild-type (EC_VASP$^{+/+}$) and VASP-deficient (EC_VASP$^{-/-}$) mice backcrossed into the C57BL/6 background for more than eight generations, were generated and cultured as previously described (Schlegel et al., 2008). Culture and transfection of HEK293 cells was carried out as described (Renne et al., 1999; Renne et al., 2005). CHO-S cells were kindly provided by Stephan M. Feller (Weatherall Institute of Molecular Medicine, University of Oxford, Oxford, UK). Adherent cultures were grown in DMEM/Ham F12 supplemented with 10% fetal calf serum. MV^{D7} cells were cultured as described (Applewhite et al., 2007).

Western blotting

To analyze VASP phosphorylation, stimulated cells were immediately lysed in SDS-sample buffer, proteins were separated by 8% SDS-PAGE under reducing conditions, and electrotransferred to a nitrocellulose membrane (Schleicher and Schüll, Dassel, Germany). Blots were probed using antibodies against 6×His-tag (Calbiochem), total-VASP (M4, Immunoglobe), S157-*P*–VASP (5C6, Nanotools; identical with 3111, Cell-Signaling Technology), S157-*P*–VASP (16C2, Nanotools), or T278-*P*–VASP (Blume et al., 2007) in 4% skimmed milk in PBS supplemented with 0.1% Tween-20, followed by horseradish-peroxidase-conjugated secondary antibodies (Dako) and chemiluminescence substrate solution (ECL Plus, Amersham Pharmacia Biotech). Expression of Mena and EVL was probed by 6×His-tag- or polyclonal Mena- or EVL-specific antibodies (Lambrechts et al., 2000). The expression of PKG variants was probed using antibodies against PKG (Smolenski et al., 2000); AMPK variants were probed by myc-tag-specific antibodies (Santa Cruz Biotechnology).

Immunocytochemistry

To localize VASP mutants in reconstituted EC_VASP$^{-/-}$, cells were cultivated in gelatinized six-well plates to 90% confluence and transiently transfected with Lipofectamine 2000 (Invitrogen). After 24 hours, cells were trypsinized, replated on gelatinized two-well chamberslides (Nunc) and cultured for an additional 3 hours. To analyze phosphorylation of endogenous VASP, sparse EC_VASP$^{+/+}$ were incubated with 5 μM forskolin for 10 minutes (Benz et al., 2008; Blume et al., 2007). All cells were washed with PBS, immediately fixed with ice-cold 4% paraformaldehyde in PBS for 5 minutes, permeabilized with 0.1% Triton X100 in PBS for 20 minutes, and blocked in 10% goat serum in PBS for 1 hour. The sections were incubated overnight with primary antibodies against total-VASP (M4), and S157-*P*–VASP (5C6), followed by secondary anti-mouse and anti-rabbit antibodies conjugated to Alexa Fluor 488 or 594 (Molecular Probes) for 1 hour. All antibody incubations were performed in 10% goat serum in PBS at room temperature. Note that the occasional nuclear staining of anti-VASP has been previously described (Benz et al., 2008; Moeller et al., 2004) and most probably represents a fixation artefact. For immunolocalization of VASP mutants in MV^{D7}, cells were transfected with Lipofectamine 2000, trypsinized after 24 hours, and replated on fibronectin-coated chamberslides for additional 2 hours before fixing and staining as detailed above. Stained sections were investigated using a NIKON Eclipse E600 microscope equipped with a C1 confocal scanning head and 100× oil immersion objective. Images were acquired and prepared for presentation using the EZ-C1 software (Nikon, version 3.00). In EC_VASP$^{-/-}$ and MV^{D7}, subcellular localization of transiently expressed VASP mutants to the leading edge of lamellipodia and focal adhesions was scored by visual inspection as weak (–), moderate (o), or strong (+). For each of the eight phosphomimetic VASP mutants, >40 cells with comparable VASP expression were randomly selected and analyzed. Localization to lamellipodia was confirmed with ARP3-specific antibodies. Ratios of VASP-positive lamellipodia and cell circumference were determined using the ImageJ (National Institutes of Health) software.

Actin polymerization assay

His_6-tagged wild-type and mutant VASP (VASP-AAA, -DAA, -ADA, -AAE, -DDA, -DAE, -ADE, and -DDE) was expressed in *E. coli* and purified as described (Bachmann et al., 1999). Proteins were quantified from Coomassie-blue-stained polyacrylamide gels by densitometric scans using bovine serum albumin (BSA) as standard (ImageJ version 1.34s). Actin polymerization assays were performed essentially as described (Harbeck et al., 2000). Briefly, 1 μM G-Actin (10% pyrene-labeled, cytoskeleton) in GA-buffer (5 mM Tris-HCl pH 8.0, 0.2 mM $CaCl_2$, 0.2 mM

ATP and 0.2 mM DTT) was mixed with or without 0.25 μM purified recombinant wild-type or mutant VASP and 58 mM imidazole, 2 mM $MgCl_2$ and 15 mM KCl to initiate actin polymerization (all final concentrations). Increase in fluorescence, representing F-actin assembly, was recorded for 9 minutes with an excitation wavelength of 366 nm and an emission wavelength of 384 nm using a PerkinElmer Life Science LS50B fluorescence photometer and the time-drive protocol of the FL Winlab 2.00 software.

SRE transcriptional reporter assays

We utilized an SRF-based transactivation assay to quantify changes in ratio of cellular G-actin to F-actin (Geneste et al., 2002; Sotiropoulos et al., 1999). HEK293 cells with low endogenous VASP and EVL expression were grown on six-well plates and transiently transfected using Rotifect (Roth, Karlsruhe, Germany). Each transfection mix (2 μg total plasmid DNA) included cDNAs coding either VASP or EVL mutants (0.1 μg), SRE reporter vector (0.5 μg, SRE-*P*; Stratagene), 0.25 μg *Renilla* luciferase transfection control vector (phRL-TK, Promega), and 1.15 μg pcDNA3 vector without insert (Invitrogen). To address the effect of kinase-mediated VASP phosphorylation, partially arrested VASP mutants were co-transfected with cDNA coding for PKGIβ (wild-type or CI) or AMPK α1 subunits (wtα, CAα, DNα). After 24 hours in serum-free medium, the cells were lysed and luciferase activity of the supernatant measured using the Dual Luciferase Reporter Assay System (Promega) with a luminometer (Lumat; Berthold Technologies, Bad Wildbad, Germany). Firefly luciferase activity was normalized to *Renilla* luciferase activity and expressed relative to mock (set to 0%) and AAA-VASP and A-EVL transfected cells (set to 100%), respectively. *Renilla* luciferase intensities did not significantly differ within cells expressing mutant VASP. To stimulate S157-VASP phosphorylation, transfected cells were incubated with 5 μM forskolin for 5, 20, 40 and 80 minutes before lysis. Transfection efficiency was controlled by immunofluorescence microscopy with a vector coding for green-fluorescent protein (GFP). Immunofluorescence microscopy revealed that more than 60% of HEK293 cells stained positive for GFP after 24 hours of expression. SRE transcriptional reporter assays with Mena mutants were performed accordingly in CHO-S cells. For transfection, Lipofectamine 2000 (Invitrogen) and 0.2 μg Mena plasmid were used. Firefly luciferase activity was normalized to *Renilla* luciferase activity and expressed relative to mock (set to 0%) and AA-Mena transfected cells (set to 100%).

Quantification of cellular F-actin content by FACS analysis

HEK293 cells were transfected using Metafectene (Biontex Laboratories, Munich, Germany) with pcDNA3 vectors coding for arrested VASP mutants (AAA, AAE, DAA, ADA, DDA, DAE, ADE, DDE; 0.25 μg each) or vector without insert (0.75 μg; Invitrogen). After 24 hours of expression in DMEM with all supplements, including serum, cells were washed with ice-cold PBS, trypsinized with ice-cold trypsin/EDTA solution, and then transferred into ice-cold DMEM containing 10% FCS to stop the trypsin/EDTA reaction. Cells were washed twice with ice-cold PBS, fixed in 3.7% paraformaldehyde in PBS (5 minutes at 4°C), permeabilized with 0.1% Triton X-100 in PBS (5 minutes at 4°C), and then fixed again in 3.7% paraformaldehyde in PBS (5 minutes at 4°C). The cells were co-stained for F-actin using Alexa-Fluor-647–phalloidin (1:250); for myc-tagged AMPK α1 subunit using anti-myc antibody (1:250); or for 6×His-tagged VASP mutants using anti-6×His antibody (1:500) followed by FITC-conjugated anti-mouse antibody (1:500; Sigma). All incubations were performed in 5% goat serum in PBS in darkness at room temperature for 1 hour. The mean cellular F-actin content determined by phalloidin staining of overexpressing cells was quantified using FACScan (BD Biosciences) as previously described (Grosse et al., 2003).

Statistical analysis

Results are expressed as mean ± s.d. Data sets were analyzed by one-way analysis of variance (ANOVA) followed by Tukey's Multiple Comparison Test to determine statistical significance between groups (Prism 3.0, GraphPad Software). Degrees of statistical significance are defined as $*P<0.05$, $**P<0.01$ and $***P<0.001$.

This work was supported in part by grants of the Deutsche Forschungsgemeinschaft (NWG SFB355/688), the EU-funded ERARE program and IZKF Würzburg, E-40 (to T.R.). K.S. was supported by the IZKF Würzburg, E-33 and the DFG (SCHU1600/2-1). F.G. acknowledges support from NIH grant GM58801. We are grateful to Stephan M. Feller for providing CHO-S cells, Daniela Urlaub for excellent technical support, and Nadja Niedermeier for help with EC_VASP cells. Deposited in PMC for release after 12 months.

References

Abel, K., Mieskes, G. and Walter, U. (1995). Dephosphorylation of the focal adhesion protein VASP in vitro and in intact human platelets. *FEBS Lett.* **370**, 184-188.

Applewhite, D. A., Barzik, M., Kojima, S., Svitkina, T. M., Gertler, F. B. and Borisy, G. G. (2007). Ena/VASP proteins have an anti-capping independent function in filopodia formation. *Mol. Biol. Cell* **18**, 2579-2591.

Bachmann, C., Fischer, L., Walter, U. and Reinhard, M. (1999). The EVH2 domain of the vasodilator-stimulated phosphoprotein mediates tetramerization, F-actin binding, and actin bundle formation. *J. Biol. Chem.* **274**, 23549-23557.

Ball, L. J., Kuhne, R., Hoffmann, B., Hafner, A., Schmieder, P., Volkmer-Engert, R., Hof, M., Wahl, M., Schneider-Mergener, J., Walter, U. et al. (2000). Dual epitope recognition by the VASP EVH1 domain modulates polyproline ligand specificity and binding affinity. *EMBO J.* **19**, 4903-4914.

Barzik, M., Kotova, T. I., Higgs, H. N., Hazelwood, L., Hanein, D., Gertler, F. B. and Schafer, D. A. (2005). Ena/VASP proteins enhance actin polymerization in the presence of barbed end capping proteins. *J. Biol. Chem.* **280**, 28653-28662.

Bear, J. E. and Gertler, F. B. (2009). Ena/VASP: towards resolving a pointed controversy at the barbed end. *J. Cell Sci.* **122**, 1947-1953.

Bear, J. E., Loureiro, J. J., Libova, I., Fassler, R., Wehland, J. and Gertler, F. B. (2000). Negative regulation of fibroblast motility by Ena/VASP proteins. *Cell* **101**, 717-728.

Bear, J. E., Svitkina, T. M., Krause, M., Schafer, D. A., Loureiro, J. J., Strasser, G. A., Maly, I. V., Chaga, O. Y., Cooper, J. A., Borisy, G. G. et al. (2002). Antagonism between Ena/VASP proteins and actin filament capping regulates fibroblast motility. *Cell* **109**, 509-521.

Benz, P. M., Blume, C., Moebius, J., Oschatz, C., Schuh, K., Sickmann, A., Walter, U., Feller, S. M. and Renne, T. (2008). Cytoskeleton assembly at endothelial cell-cell contacts is regulated by alphaII-spectrin-VASP complexes. *J. Cell Biol.* **180**, 205-219.

Blume, C., Benz, P. M., Walter, U., Ha, J., Kemp, B. E. and Renne, T. (2007). AMP-activated protein kinase impairs endothelial actin cytoskeleton assembly by phosphorylating vasodilator-stimulated phosphoprotein. *J. Biol. Chem.* **282**, 4601-4612.

Butt, E., Abel, K., Krieger, M., Palm, D., Hoppe, V., Hoppe, J. and Walter, U. (1994). cAMP- and cGMP-dependent protein kinase phosphorylation sites of the focal adhesion vasodilator-stimulated phosphoprotein (VASP) in vitro and in intact human platelets. *J. Biol. Chem.* **269**, 14509-14517.

Chen, L., Daum, G., Chitaley, K., Coats, S. A., Bowen-Pope, D. F., Eigenthaler, M., Thumati, N. R., Walter, U. and Clowes, A. W. (2004). Vasodilator-stimulated phosphoprotein regulates proliferation and growth inhibition by nitric oxide in vascular smooth muscle cells. *Arterioscler Thromb. Vasc. Biol.* **24**, 1403-1408.

Comerford, K. M., Lawrence, D. W., Synnestvedt, K., Levi, B. P. and Colgan, S. P. (2002). Role of vasodilator-stimulated phosphoprotein in PKA-induced changes in endothelial junctional permeability. *FASEB J.* **16**, 583-585.

Dephoure, N., Zhou, C., Villen, J., Beausoleil, S. A., Bakalarski, C. E., Elledge, S. J. and Gygi, S. P. (2008). A quantitative atlas of mitotic phosphorylation. Proc. Natl. Acad. Sci. USA **105**, 10762-10767.

Ferron, F., Rebowski, G., Lee, S. H. and Dominguez, R. (2007). Structural basis for the recruitment of profilin-actin complexes during filament elongation by Ena/VASP. *EMBO J* **26**, 4597-4606.

Furman, C., Sieminski, A. L., Kwiatkowski, A. V., Rubinson, D., Vasile, E., Bronson, R. T., Fässler, R. and Gertler, F. B. (2007). Ena/VASP is required for endothelial barrier function in vivo. *J. Cell Biol.* **179**, 761-775.

Gachet, C. and Aleil, B. (2008). Testing antiplatelet therapy. *Eur. Heart J.* **Suppl. 10** A28-A34.

Geese, M., Loureiro, J. J., Bear, J. E., Wehland, J., Gertler, F. B. and Sechi, A. S. (2002). Contribution of Ena/VASP proteins to intracellular motility of listeria requires phosphorylation and proline-rich core but not F-actin binding or multimerization. *Mol. Biol. Cell* **13**, 2383-2396.

Geneste, O., Copeland, J. W. and Treisman, R. (2002). LIM kinase and Diaphanous cooperate to regulate serum response factor and actin dynamics. *J. Cell Biol.* **157**, 831-838.

Gertler, F. B., Niebuhr, K., Reinhard, M., Wehland, J. and Soriano, P. (1996). Mena, a relative of VASP and Drosophila Enabled, is implicated in the control of microfilament dynamics. *Cell* **87**, 227-239.

Grosse, R., Copeland, J. W., Newsome, T. P., Way, M. and Treisman, R. (2003). A role for VASP in RhoA-Diaphanous signalling to actin dynamics and SRF activity. *EMBO J.* **22**, 3050-3061.

Halbrugge, M., Friedrich, C., Eigenthaler, M., Schanzenbacher, P. and Walter, U. (1990). Stoichiometric and reversible phosphorylation of a 46-kDa protein in human platelets in response to cGMP- and cAMP-elevating vasodilators. *J Biol. Chem.* **265**, 3088-3093.

Han, Y. H., Chung, C. Y., Wessels, D., Stephens, S., Titus, M. A., Soll, D. R. and Firtel, R. A. (2002). Requirement of a vasodilator-stimulated phosphoprotein family member for cell adhesion, the formation of filopodia, and chemotaxis in dictyostelium. *J. Biol. Chem.* **277**, 49877-49887.

Harbeck, B., Huttelmaier, S., Schluter, K., Jockusch, B. M. and Illenberger, S. (2000). Phosphorylation of the vasodilator-stimulated phosphoprotein regulates its interaction with actin. *J. Biol. Chem.* **275**, 30817-30825.

Howe, A. K., Hogan, B. P. and Juliano, R. L. (2002). Regulation of vasodilator-stimulated phosphoprotein phosphorylation and interaction with Abl by protein kinase A and cell adhesion. *J. Biol. Chem.* **277**, 38121-38126.

Kouyama, T. and Mihashi, K. (1981). Fluorimetry study of N-(1-pyrenyl)iodoacetamide-labelled F-actin. Local structural change of actin protomer both on polymerization and on binding of heavy meromyosin. *Eur. J. Biochem.* **114**, 33-38.

Krause, M., Dent, E. W., Bear, J. E., Loureiro, J. J. and Gertler, F. B. (2003). Ena/VASP proteins: regulators of the actin cytoskeleton and cell migration. *Annu. Rev. Cell Dev. Biol.* **19**, 541-564.

Kuhnel, K., Jarchau, T., Wolf, E., Schlichting, I., Walter, U., Wittinghofer, A. and Strelkov, S. V. (2004). The VASP tetramerization domain is a right-handed coiled coil based on a 15-residue repeat. *Proc. Natl. Acad. Sci. USA* **101**, 17027-17032.

Kwiatkowski, A. V., Gertler, F. B. and Loureiro, J. J. (2003). Function and regulation of Ena/VASP proteins. *Trends Cell Biol.* **13**, 386-392.
Lambrechts, A., Kwiatkowski, A. V., Lanier, L. M., Bear, J. E., Vandekerckhove, J., Ampe, C. and Gertler, F. B. (2000). cAMP-dependent protein kinase phosphorylation of EVL, a Mena/VASP relative, regulates its interaction with actin and SH3 domains. *J. Biol. Chem.* **275**, 36143-36151.
Laurent, V., Loisel, T. P., Harbeck, B., Wehman, A., Grobe, L., Jockusch, B. M., Wehland, J., Gertler, F. B. and Carlier, M. F. (1999). Role of proteins of the Ena/VASP family in actin-based motility of Listeria monocytogenes. *J. Cell Biol.* **144**, 1245-1258.
Lawrence, D. W. and Pryzwansky, K. B. (2001). The vasodilator-stimulated phosphoprotein is regulated by cyclic GMP-dependent protein kinase during neutrophil spreading. *J. Immunol.* **166**, 5550-5556.
Lindsay, S. L., Ramsey, S., Aitchison, M., Renne, T. and Evans, T. J. (2007). Modulation of lamellipodial structure and dynamics by NO-dependent phosphorylation of VASP Ser239. *J. Cell Sci.* **120**, 3011-3021.
Loureiro, J. J., Rubinson, D. A., Bear, J. E., Baltus, G. A., Kwiatkowski, A. V. and Gertler, F. B. (2002). Critical roles of phosphorylation and actin binding motifs, but not the central proline-rich region, for Ena/vasodilator-stimulated phosphoprotein (VASP) function during cell migration. *Mol. Biol. Cell* **13**, 2533-2546.
Maekawa, M., Ishizaki, T., Boku, S., Watanabe, N., Fujita, A., Iwamatsu, A., Obinata, T., Ohashi, K., Mizuno, K. and Narumiya, S. (1999). Signaling from Rho to the actin cytoskeleton through protein kinases ROCK and LIM-kinase. *Science* **285**, 895-898.
Martin, K. H., Jeffery, E. D., Grigera, P. R., Shabanowitz, J., Hunt, D. F. and Parsons, J. T. (2006). Cortactin phosphorylation sites mapped by mass spectrometry. *J. Cell Sci.* **119**, 2851-2853.
Mitchison, T. J. and Cramer, L. P. (1996). Actin-based cell motility and cell locomotion. *Cell* **84**, 371-379.
Moeller, M. J., Soofi, A., Braun, G. S., Li, X., Watzl, C., Kriz, W. and Holzman, L. B. (2004). Protocadherin FAT1 binds Ena/VASP proteins and is necessary for actin dynamics and cell polarization. *EMBO J.* **23**, 3769-3779.
Munzel, T., Feil, R., Mulsch, A., Lohmann, S. M., Hofmann, F. and Walter, U. (2003). Physiology and pathophysiology of vascular signaling controlled by guanosine 3′,5′-cyclic monophosphate-dependent protein kinase. *Circulation* **108**, 2172-2183.
Neel, N. F., Barzik, M., Raman, D., Sobolik-Delmaire, T., Sai, J., Ham, A. J., Mernaugh, R. L., Gertler, F. B. and Richmond, A. (2009). VASP is a CXCR2-interacting protein that regulates CXCR2-mediated polarization and chemotaxis. *J. Cell Sci.* **122**, 1882-1894.
Pasic, L., Kotova, T. and Schafer, D. A. (2008). Ena/VASP proteins capture actin filament barbed ends. *J. Biol. Chem.* **283**, 9814-9819.
Price, C. J. and Brindle, N. P. (2000). Vasodilator-stimulated phosphoprotein is involved in stress-fiber and membrane ruffle formation in endothelial cells. *Arterioscler Thromb Vasc. Biol.* **20**, 2051-2056.
Profirovic, J., Gorovoy, M., Niu, J., Pavlovic, S. and Voyno-Yasenetskaya, T. (2005). A novel mechanism of G protein-dependent phosphorylation of vasodilator-stimulated phosphoprotein. *J. Biol. Chem.* **280**, 32866-32876.
Pula, G., Schuh, K., Nakayama, K., Nakayama, K. I., Walter, U. and Poole, A. W. (2006). PKCdelta regulates collagen-induced platelet aggregation through inhibition of VASP-mediated filopodia formation. *Blood* **108**, 4035-4044.
Reinhard, M., Giehl, K., Abel, K., Haffner, C., Jarchau, T., Hoppe, V., Jockusch, B. M. and Walter, U. (1995). The proline-rich focal adhesion and microfilament protein VASP is a ligand for profilins. *EMBO J.* **14**, 1583-1589.
Renne, T., Dedio, J., Meijers, J. C., Chung, D. and Müller-Esterl, W. (1999). Mapping of the discontinuous H-kininogen binding site of plasma prekallikrein. Evidence for a critical role of apple domain-2. *J. Biol. Chem.* **274**, 25777-25784.
Renne, T., Schuh, K. and Muller-Esterl, W. (2005). Local bradykinin formation is controlled by glycosaminoglycans. *J. Immunol.* **175**, 3377-3385.
Rentsendorj, O., Mirzapoiazova, T., Adyshev, D., Servinsky, L. E., Renne, T., Verin, A. D. and Pearse, D. B. (2008). Role of vasodilator-stimulated phosphoprotein in cGMP-mediated protection of human pulmonary artery endothelial barrier function. *Am. J. Physiol. Lung Cell Mol. Physiol.* **294**, L686-L697.
Rikova, K., Guo, A., Zeng, Q., Possemato, A., Yu, J., Haack, H., Nardone, J., Lee, K., Reeves, C., Li, Y. et al. (2007). Global survey of phosphotyrosine signaling identifies oncogenic kinases in lung cancer. *Cell* **131**, 1190-1203.
Rosenberger, P., Khoury, J., Kong, T., Weissmuller, T., Robinson, A. M. and Colgan, S. P. (2007). Identification of vasodilator-stimulated phosphoprotein (VASP) as an HIF-regulated tissue permeability factor during hypoxia. *FASEB J.* **21**, 2613-2621.
Sandberg, M., Natarajan, V., Ronander, I., Kalderon, D., Walter, U., Lohmann, S. M. and Jahnsen, T. (1989). Molecular cloning and predicted full-length amino acid sequence of the type I beta isozyme of cGMP-dependent protein kinase from human placenta. Tissue distribution and developmental changes in rat. *FEBS Lett.* **255**, 321-329.
Schirenbeck, A., Arasada, R., Bretschneider, T., Stradal, T. E., Schleicher, M. and Faix, J. (2006). The bundling activity of vasodilator-stimulated phosphoprotein is required for filopodium formation. *Proc. Natl. Acad. Sci. USA* **103**, 7694-7969.
Schlegel, N., Burger, S., Golenhofen, N., Walter, U., Drenckhahn, D. and Waschke, J. (2008). The role of VASP in regulation of cAMP- and Rac 1-mediated endothelial barrier stabilization. *Am. J. Physiol. Cell Physiol.* **294**, C178-C188.
Schmidt, A. and Hall, M. N. (1998). Signaling to the actin cytoskeleton. *Annu. Rev. Cell Dev. Biol.* **14**, 305-338.
Sechi, A. S. and Wehland, J. (2004). ENA/VASP proteins: multifunctional regulators of actin cytoskeleton dynamics. *Front Biosci.* **9**, 1294-1310.
Skoble, J., Auerbuch, V., Goley, E. D., Welch, M. D. and Portnoy, D. A. (2001). Pivotal role of VASP in Arp2/3 complex-mediated actin nucleation, actin branch-formation, and Listeria monocytogenes motility. *J. Cell Biol.* **155**, 89-100.
Smolenski, A., Poller, W., Walter, U. and Lohmann, S. M. (2000). Regulation of human endothelial cell focal adhesion sites and migration by cGMP-dependent protein kinase I. *J. Biol. Chem.* **275**, 25723-25732.
Sotiropoulos, A., Gineitis, D., Copeland, J. and Treisman, R. (1999). Signal-regulated activation of serum response factor is mediated by changes in actin dynamics. *Cell* **98**, 159-169.
Suzuki, J., Fukuda, M., Kawata, S., Maruoka, M., Kubo, Y., Takeya, T. and Shishido, T. (2006). A rapid protein expression and purification system using Chinese hamster ovary cells expressing retrovirus receptor. *J. Biotechnol.* **126**, 463-474.
Trichet, L., Sykes, C. and Plastino, J. (2008). Relaxing the actin cytoskeleton for adhesion and movement with Ena/VASP. *J. Cell Biol.* **181**, 19-25.
Vasioukhin, V., Bauer, C., Yin, M. and Fuchs, E. (2000). Directed actin polymerization is the driving force for epithelial cell-cell adhesion. *Cell* **100**, 209-219.
Wentworth, J. K., Pula, G. and Poole, A. W. (2006). Vasodilator-stimulated phosphoprotein (VASP) is phosphorylated on Ser157 by protein kinase C-dependent and -independent mechanisms in thrombin-stimulated human platelets. *Biochem. J.* **393**, 555-564.
Woods, A., Azzout-Marniche, D., Foretz, M., Stein, S. C., Lemarchand, P., Ferre, P., Foufelle, F. and Carling, D. (2000). Characterization of the role of AMP-activated protein kinase in the regulation of glucose-activated gene expression using constitutively active and dominant negative forms of the kinase. *Mol. Cell. Biol.* **20**, 6704-6711.
Zahedi, R. P., Lewandrowski, U., Wiesner, J., Wortelkamp, S., Moebius, J., Schutz, C., Walter, U., Gambaryan, S. and Sickmann, A. (2008). Phosphoproteome of resting human platelets. *J. Proteome Res.* **7**, 526-534.
Zhang, X., Yuan, Z., Zhang, Y., Yong, S., Salas-Burgos, A., Koomen, J., Olashaw, N., Parsons, J. T., Yang, X. J., Dent, S. R. et al. (2007). HDAC6 modulates cell motility by altering the acetylation level of cortactin. *Mol. Cell* **27**, 197-213.
Zhuang, S., Nguyen, G. T., Chen, Y., Gudi, T., Eigenthaler, M., Jarchau, T., Walter, U., Boss, G. R. and Pilz, R. B. (2004). Vasodilator-stimulated phosphoprotein activation of serum-response element-dependent transcription occurs downstream of RhoA and is inhibited by cGMP-dependent protein kinase phosphorylation. *J. Biol. Chem.* **279**, 10397-10407.

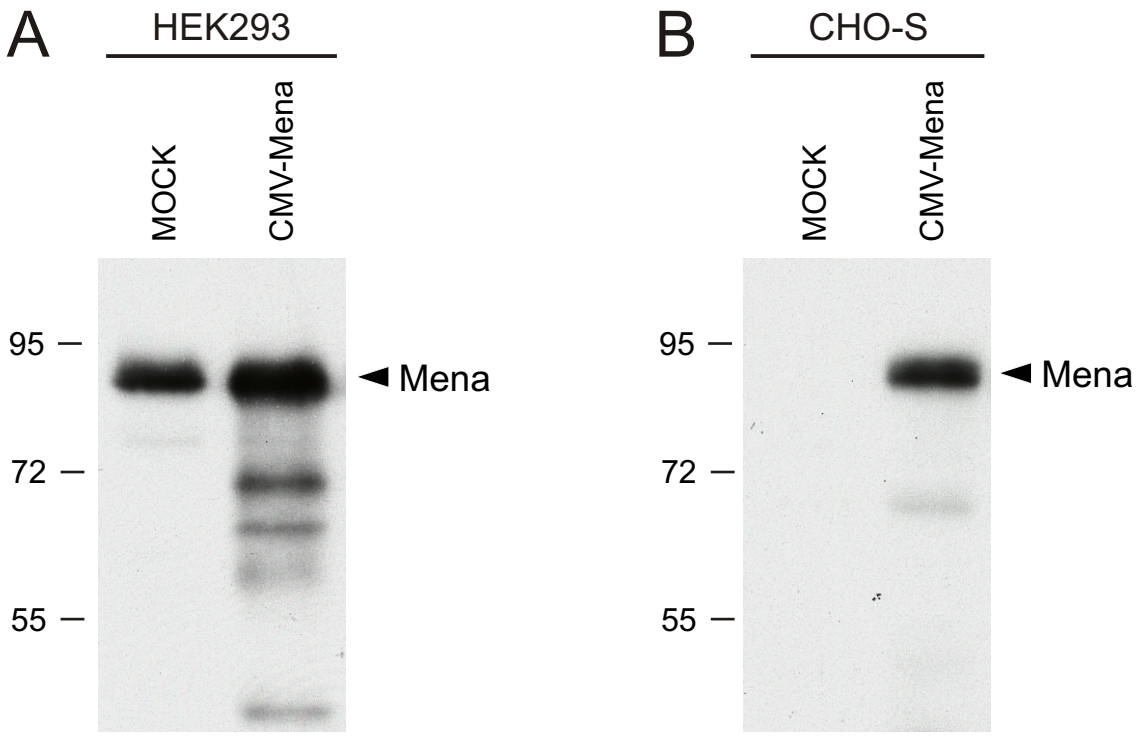
A
HEK293
MOCK
CMV-Mena
95
72
55
Mena
B
CHO-S
MOCK
CMV-Mena
95
72
55
Mena

Supplemental Table 1. Primers for the introduction of Ena/VASP pointmutations	
VASP	Primer Sequence
S157A	5´- CG GAG CAC ATA GAG CGC CGG GTC GCC AAT GCA GGA GGC CCA CC - 3´
S157D	5´- CG GAG CAC ATA GAG CGC CGG GTC GAC AAT GCA GGA GGC CCA CC - 3´
S239A	5´- GGA GCC AAA CTC AGG AAA GTC GCC AAG CAG GAG GAG GCC TCA GGG - 3´
S239D	5´- GGA GCC AAA CTC AGG AAA GTC GAC AAG CAG GAG GAG GCC TCA GGG - 3´
T278A	5´- G CTG GCC CGG AGA AGG AAA GCC GCG CAA GTT GGG GAG AAA ACC - 3´
T278E	5´- G CTG GCC CGG AGA AGG AAA GCC GAG CAA GTT GGG GAG AAA ACC - 3´
Mena*	Primer Sequence
A236D	5´- A GAG CGC AGA ATG GAC AAT GCT GCT GCC C - 3´
A376D	5´- AA CTT AGG AAA GTG GAC CGG GTG GAG GAT GG - 3´
EVL	Primer Sequence
S160A	5´- GG AAT CTC TAG AAA AGA AGA ACC GCC GCC ACA GGC CCA TCC TCC C - 3´
S160D	5´- GG AAT CTC TAG AAA AGA AGA ACC GAC GCC ACA GGC CCA TCC TCC C - 3´

* Phosphomimetic murine Mena mutants AA and DD were kindly provided by FG and subcloned into pcDNA3 vector.